

UCLA

UCLA Previously Published Works

Title

Radial mobility and cytotoxic function of retroviral replicating vector transduced, non-adherent alloresponsive T lymphocytes.

Permalink

<https://escholarship.org/uc/item/3475z90f>

Authors

Erickson, Kate L

Hickey, Michelle J

Kato, Yuki

et al.

Publication Date

2015

DOI

10.3791/52416

Peer reviewed

Video Article

Radial Mobility and Cytotoxic Function of Retroviral Replicating Vector Transduced, Non-adherent Alloresponsive T Lymphocytes

Kate L. Erickson^{*1}, Michelle J. Hickey^{*1}, Yuki Kato², Colin C. Malone¹, Geoffrey C. Owens¹, Robert M. Prins^{1,2}, Linda M. Liau^{1,4,5}, Noriyuki Kasahara^{3,5}, Carol A. Kruse^{1,4,5}

¹Department of Neurosurgery, UCLA David Geffen School of Medicine

²Department of Molecular and Medical Pharmacology, UCLA David Geffen School of Medicine

³Department of Medicine, UCLA David Geffen School of Medicine

⁴Brain Research Institute, UCLA David Geffen School of Medicine

⁵Jonsson Comprehensive Cancer Center, UCLA David Geffen School of Medicine

*These authors contributed equally

Correspondence to: Carol A. Kruse at ckruse@mednet.ucla.edu

URL: <http://www.jove.com/video/52416>

DOI: [doi:10.3791/52416](https://doi.org/10.3791/52416)

Keywords: Immunology, Issue 96, non-adherent cell migration, fluorescence microscopy, cell sedimentation manifold, allogeneic CTL, monolayer, T cell, extracellular matrix, gliom

Date Published: 2/11/2015

Citation: Erickson, K.L., Hickey, M.J., Kato, Y., Malone, C.C., Owens, G.C., Prins, R.M., Liau, L.M., Kasahara, N., Kruse, C.A. Radial Mobility and Cytotoxic Function of Retroviral Replicating Vector Transduced, Non-adherent Alloresponsive T Lymphocytes. *J. Vis. Exp.* (96), e52416, doi:10.3791/52416 (2015).

Abstract

We report a novel adaptation of the Radial Monolayer Cell Migration assay, first reported to measure the radial migration of adherent tumor cells on extracellular matrix proteins, for measuring the motility of fluorescently-labeled, non-adherent human or murine effector immune cells. This technique employs a stainless steel manifold and 10-well Teflon slide to focally deposit non-adherent T cells into wells prepared with either confluent tumor cell monolayers or extracellular matrix proteins. Light and/or multi-channel fluorescence microscopy is used to track the movement and behavior of the effector cells over time. Fluorescent dyes and/or viral vectors that code for fluorescent transgenes are used to differentially label the cell types for imaging. This method is distinct from similar-type *in vitro* assays that track horizontal or vertical migration/ invasion utilizing slide chambers, agar or transwell plates. The assay allows detailed imaging data to be collected with different cell types distinguished by specific fluorescent markers; even specific subpopulations of cells (*i.e.*, transduced/nontransduced) can be monitored. Surface intensity fluorescence plots are generated using specific fluorescence channels that correspond to the migrating cell type. This allows for better visualization of the non-adherent immune cell mobility at specific times. It is possible to gather evidence of other effector cell functions, such as cytotoxicity or transfer of viral vectors from effector to target cells, as well. Thus, the method allows researchers to microscopically document cell-to-cell interactions of differentially-labeled, non-adherent with adherent cells of various types. Such information may be especially relevant in the assessment of biologically-manipulated or activated immune cell types, where visual proof of functionality is desired with tumor target cells before their use for cancer therapy.

Video Link

The video component of this article can be found at <http://www.jove.com/video/52416/>

Introduction

The Radial Monolayer Cell Migration assay was originally developed to measure the infiltrative properties of adherent tumor cells¹⁻⁴ on slides coated with extracellular matrix (ECM) proteins⁵⁻⁷ or with individual ECM components, such as fibronectin or laminin^{1,2}. The technique involved seeding a single cell suspension of tumor cells in the center of wells using a stainless steel cell sedimentation manifold (CSM). After sedimentation, the tumor cells would adhere to the bottom of the well and the change in the diameter of the initial cell population over time was used to establish a rate of horizontal motility. The Radial Monolayer Cell Migration assay provided a visual advantage over other existing methods that employed transwell plates to assay the *in vitro* migratory capabilities of cells; these assays are non-conductive to imaging⁸. As well, it also provided a great amount of freedom in choosing the timepoints when migration is assessed, with no limit on the number of timepoints a researcher could choose to image after sedimentation.

Because the ability to migrate is an important functionality for non-adherent cells, especially in the area of immunotherapy or where they may be used as delivery vehicles for viral vectors, we adapted the use of the CSM to evaluate the migration of non-adherent cell types on tumor cell monolayers, in addition to ECM proteins. The added benefit of microscopically visualizing the migration of non-adherent cells on viable tumor cell monolayers, on complex ECM isolated from the tumor, or on individual ECM components makes this assay versatile. Assays that employ wells coated with a single extracellular protein do not reflect accurately the ECM tissue substrate or tumor the cells would migrate through *in vivo*.

Here, we used alloreactive cytotoxic T lymphocytes (alloCTL), sensitized to major histocompatibility complex (MHC) proteins using one-way mixed lymphocyte tumor cell reactions (MLTR) or mixed lymphocyte reactions (MLR)⁹, as our representative non-adherent cell type. We tested cells of both human and murine origin. When migration was measured on tumor monolayers, the tumor cells employed were either partially relevant targets, displaying some of the same MHC proteins found on the cell population used to sensitize the effectors, or fully relevant targets, with a full set of MHC molecules that the effectors had been sensitized towards. In some experiments, we used fluorescent CellTracker Red CMPTX or cell proliferation dye eFluor 670 to differentiate between effector and target cells. We also used transduction with viral vectors encoding for fluorescent proteins as an additional way to visualize the cells. For certain assays, we transduced the alloCTL with retroviral replicating vectors (RRV) coding for Emerald Green (EMD) fluorescent protein^{10,11}; for others, tumor cells were transduced with lentiviral vectors coding for mStrawberry.

The alloCTL were seeded through a channel of the manifold into the center of either tumor cell monolayers or ECM harvested from tumor cell monolayers. Adherent and non-adherent cell interactions were visualized by light and/or by fluorescence microscopy over time. Disruption in the tumor cell monolayer at low power, or tumor cells with fragmented nuclei at high power were indicators of cell injury by lysis and apoptosis, respectively. We digitally created surface intensity fluorescent maps showing the migration of non-adherent fluorescing T cells over the monolayer cultures. We also noted the cytotoxicity engendered to the adherent glioma cell monolayer after cluster formation of the overlaid non-adherent alloCTL. As well, horizontal transduction of RRV-EMD from the alloCTL to the glioma monolayer was observed.

Protocol

1. Slide Preparation

1. Insert Cell Sedimentation Manifold slides into sterilization pouches and seal with autoclave tape. Face the Teflon-coated side of the slide the paper-side of the pouch to avoid plastic deposits on the wells.
2. Autoclave pouches for 15 min at 121 °C.
3. Remove slide from sterilization pouch inside a biosafety cabinet and place in a sterile 150 x 15 mm sterile Petri dish. Up to four slides can fit per dish. Place a 35 x 10 mm Petri dish next to the slides. Add 2-3 ml of sterile H₂O to provide humidification.
4. Pre-coat slides with poly-D-lysine at 100 µg/ml by using enough volume to cover the entire well. After one hr at RT, aspirate the solution and rinse the surface of the well twice by pipetting 1x PBS over the surface of the wells.
5. Optionally, add fibronectin or other ECM components to ensure stronger tumor cell adherence. Add fibronectin at 5 µg/ml in enough volume that the wells will not dry within a short period of time at RT.
 1. After 1 hr, aspirate the leftover solution and wash twice by pipetting up and down with 1x PBS.
6. Keep PBS on the wells until tumor is ready for plating. Use slides the same day.
7. Harvest a confluent flask of the desired adherent tumor cell type. Count viable cells using Trypan Blue dye exclusion by light microscopy and resuspend at 5×10^6 cells/ml in adequately-buffered growth medium—for example, Dulbecco's minimal essential medium (DMEM) with 10% fetal bovine serum (FBS), L-glutamine and sodium pyruvate.
8. If fluorescent imaging of the adherent cell population is desired, label the adherent cell population with a vital fluorescent dye or a cell proliferation dye by following the protocols provided by the manufacturer.
9. Smoothly pipette 10 µl of complete medium into each well of the slide taking care to avoid creating bubbles in the wells, as these can prevent uniform tumor cell adherence.
10. Add $2.5\text{--}5.0 \times 10^4$ cells (5-10 µl of cell suspension) to the medium in each well (**Figure 1A**). Adjust the optimal number depending on tumor cell type and the number of days of growth desired. Larger tumor cells or fast growing cells may require fewer cells initially. Bring well volume up to 40 µl by adding medium and pipette up and down to ensure an even distribution of cells.
11. After all wells are seeded, allow the tumor cells to adhere at RT, then place the lid on the 150 x 15 mm Petri dish and carefully move the dish to a 37 °C/5% CO₂ humidified incubator for at least 24 hr.
12. Change the culture medium daily. Carefully pipette a portion of the spent medium from the monolayer and replace with fresh complete medium.

NOTE: Because of evaporation, more volume will need to be added than was taken out. Wells will be ready for assay when an even, confluent layer of cells is present. This is typically 1-3 days after initial seeding.
13. Wash monolayer gently once with PBS as described in step 1.4 and either proceed to step 2 if monolayers are desired, or to step 1.13 below to extract ECM proteins from the monolayer.
14. Make a 0.5% Triton-X (v/v) solution in complete medium and add 30 µl to each well. Let monolayer digest in hood for 2 min, then wash twice with complete medium by pipetting as described above.

NOTE: The ECM layer may be visible by light microscopy (**Figure 2**). Use slides right away, or keep in complete medium in the humidified CO₂ incubator for 1-2 days. Do not allow wells to dry out.

2. Sedimentation of Non-adherent T Cells onto Slide

1. If fluorescent imaging of the non-adherent cell population is desired, label the non-adherent cell populations with a vital fluorescent dye, such as CFSE, Cell Tracker Red CMPTX, or eFluor 670 by following the protocols provided by the manufacturer at least 1 hr in advance of the assay. Alternatively, manipulate cells to express fluorescent proteins encoded by viral vectors.
2. Autoclave the cell sedimentation manifold in an autoclave pouch as described in 1.2 above.
3. Remove the humidified chamber containing Teflon coated slides from the incubator and place in biological safety cabinet.
4. Wash wells with 1x PBS by pipetting up and down, then add 45 µl of complete medium containing at least 10% serum.
5. Remove the manifold from the sterilization envelope and carefully slide in over the wells until the 'hook' at the end of the manifold touches the bottom of the slide (**Figure 1B**).
6. Ensure that the culture medium is visible in each of the channels. If none is seen, take off the manifold and add more medium to the corresponding well, then replace and check again.

7. Repeat step 2.5 for each channel of the manifold, or for as many wells as desired.
8. Count non-adherent cells and resuspend at no less than $1.0\text{-}2.0 \times 10^5/\mu\text{l}$. Draw up $1 \mu\text{l}$ of cells and slowly pipette them into the channel (**Figure 1C**). Do this for each well desired.
9. Leave the entire cell loaded apparatus, *i.e.*, manifold and slide, inside the bio-hood for 20-30 min to allow the cells in the channel to settle.
10. Remove the manifold by touching both ends and gently lifting it straight up from the slide so as to not disturb the cells focally seeded in the center of the wells (**Figure 1D**).
11. Inspect each well to ensure that the non-adherent cells have been successfully seeded at the center of the well staying within the circumference of the manifold channel. The non-adherent cells will ideally slightly adhere to the monolayer or ECM and to each other, therefore gently moving the slide around will not cause the cell pellet to disperse. Do not jostle the slide.

3. Fluorescence Microscopy

1. With appropriate experimental equipment, perform the imaging after sedimentation is confirmed. Ideally, use a microscope that is equipped with a CO₂ and humidity chamber. Image at low power, *i.e.*, 4X or 10X, to allow for multiple images to be taken of a larger area so that the entirety of the well can be seen.
2. Acquire digital images using image capture software. Perform brightfield and/or multi-channel fluorescence imaging.
3. If desired, set up a time-lapse to record images in different channels over a given area, or keep the slide humidified and in a 37 °C/5% CO₂ incubator and manually take out to image at the time points desired (**Figure 1E & F**, recommended for longer time points).

4. Analysis and Display

1. Using image editing software, merge light and fluorescent images into one layer so multiple cell types and markers can be seen in the same image. Drag and drop the image files for each individual color into the program and, when prompted, select the 'Add Layer' option to create an image file with multiple layers.
 1. At higher magnification, take, align, and stitch together images across the well digitally. Align files by looking at conserved regions between two images and overlaying one image on top of the other until a complete picture is generated.
2. Add micron bars to images during acquisition using the capture software to determine distance individual cells have migrated.
3. To determine the cell migration at various times, make surface intensity fluorescence maps with image software, *i.e.*, ImageJ, to quantify fluorescent T cell aggregation or spread over time.
 1. To generate surface plots, take a layered image generated in step 4.1 and under the Layers window, uncheck all layers except the ones corresponding to the channel desired. For instance, if a surface plot is desired to visualize EMD expression, only the 'green' layers corresponding to the filter used for this marker should be visible.
 2. Flatten the image and save it in a file format recognized (*e.g.*, .png) and load the image into the program. To generate the surface plot, change the image type to 8-bit, change the brightness/contrast as needed to reduce background, and select the 'Analyze/Surface Plot' option. The images in **Figure 5** were generated by checking the 'Shade', 'Draw Axis', 'One Polygon Per Line', and 'Smooth' checkboxes.
 3. Alternatively, take measurements using the radius or diameter from the focal cell deposit at time zero and compare to the cells at the outermost point at different times. The diameter of the Teflon wells is 6.0 mm.

Representative Results

Viral vectors encoding for fluorescent proteins can be used in addition to, or instead of, fluorescent dye. Viral transduction should be performed in advance of the motility assay. Both adherent and non-adherent cell types can be differentially-labeled. The protocol for transduction will depend on the type of vector employed. Here, we transduced the alloCTL in **Figures 3, 5 and 6** with RRV-EMD at least two days in advance of the assay using the protocol described¹². We also used a lentiviral vector, CMV-Strawberry-IRES-FLUC2, to transduce the tumor cells to express the mStrawberry red fluorescent protein (**Figure 4**). This transduction was accomplished by adding the vector to the flask of cells for 48 hr, at which point, fresh medium was added. After allowing the cells to recover for two days, limiting dilution was performed to generate a population of 100% transduced cells.

Human alloCTL were made with inactivated stimulator human 13-06-MG malignant glioma cells by MLTR. The alloCTL then were transduced with RRV coding for EMD (RRV-EMD) and later seeded into the center of established monolayers of U-87MG glioma cells with partial MHC-match to 13-06-MG (**Figures 3 and 5**). Fluorescence microscopy shows cells, initially seeded at the center of the well, migrate away from the center over time. The formation of alloCTL aggregates after 4 hr (**Figure 3**, white arrows) is likely reflective of autocrine growth patterns exhibited by activated, IL-2-producing T cell populations¹³.

In another experiment, murine effector alloCTL were made by one-way MLR using haplotype H-2d Balb/c responder splenocytes and haplotype H-2b/k stimulator splenocytes from B6C3F1 mice, the strain to which the TU-2449 glioma is syngeneic. Immediately before seeding through the channel of the manifold onto the tumor cell monolayer, the alloCTL were stained with eFluor 670. The alloCTL (purple cells) were seeded into the center of established monolayers of TU-2449 glioma cells (red) that were 100% transduced with the CMV-Straw-IRES-FLUC2 viral vector, and plated on wells the day before assay. **Figure 4A and B** show microscopic images taken of the same quadrant of the same well at 1 and 48 hr. **Figure 4C and D** were generated using ImageJ to convert digitized purple fluorescence intensities into quantitative surface plots that are displayed in three-dimensional format.

Finally, human alloCTL were made with inactivated stimulator human brain-tropic cells derived from the metastatic breast tumor cell line MDA-MB-231BR by MLTR. **Figure 6** shows light and fluorescence microscopy images over time of non-adherent CMPTX-labeled alloCTL, partially transduced with RRV-EMD, migrating on ECM proteins extracted from those tumor cells. In (**A**) the bright field photomicrograph shows focal

placement of alloCTL immediately after sedimentation. In (B and F) bright field photomicrographs show, at 4 and 8 hr, respectively, the alloCTL radially migrating on the ECM. The alloCTL density decreases with distance from the center of the well (center of well is top left corner of field in B-I). Panels (C and G) show the entire alloCTL preparation stained with CMTPIX; (D and H) show partial transduction of the alloCTL with RRV-EMD as indicated by small numbers of EMD+ T cells, and (E and I) show the merged images of the RRV-EMD transduced alloCTL migrating on the ECM along with the untransduced alloCTL.

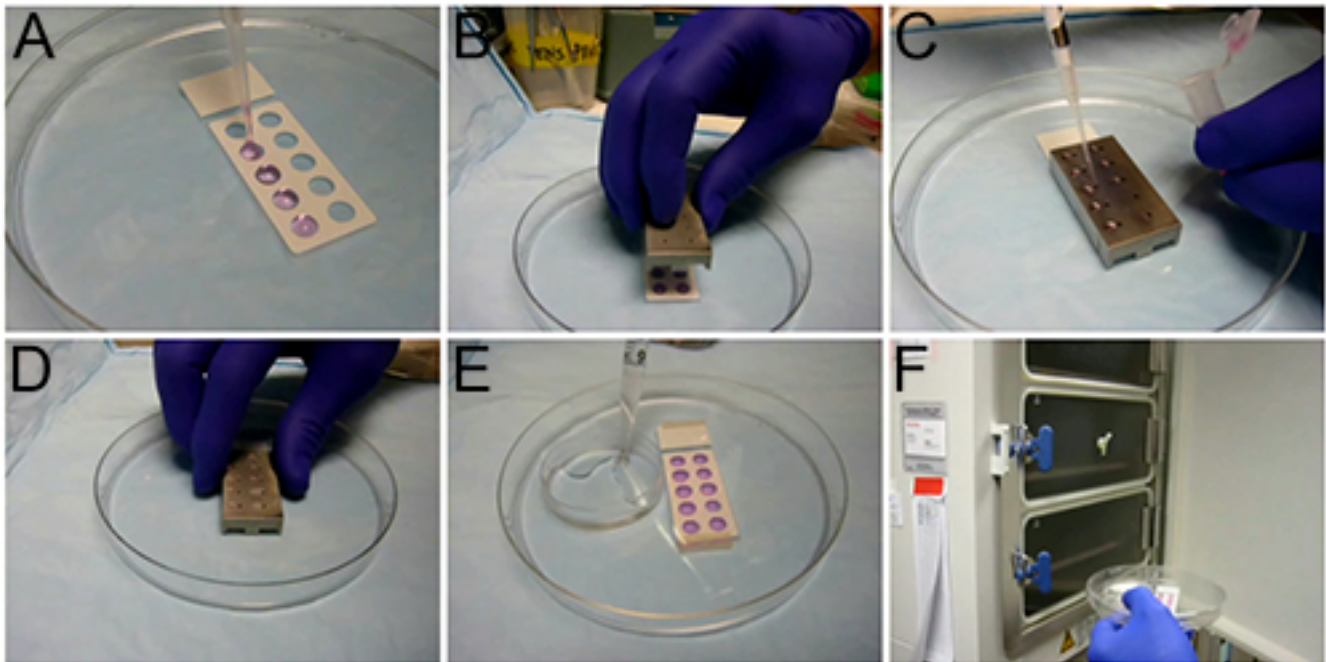


Figure 1. Cell sedimentation process. (A) Wells being prepared for sedimentation, (B) a cell sedimentation manifold placed on a slide, (C) non-adherent effector lymphocytes being loaded into the manifold, (D) manual removal of the cell sedimentation manifold, (E) a humidity chamber, (F) slides being placed in humidified incubator. This figure is used with copyright permission from Creative Scientific (<http://www.creative-sci.com/>). [Click here for a larger version of this figure.](#)

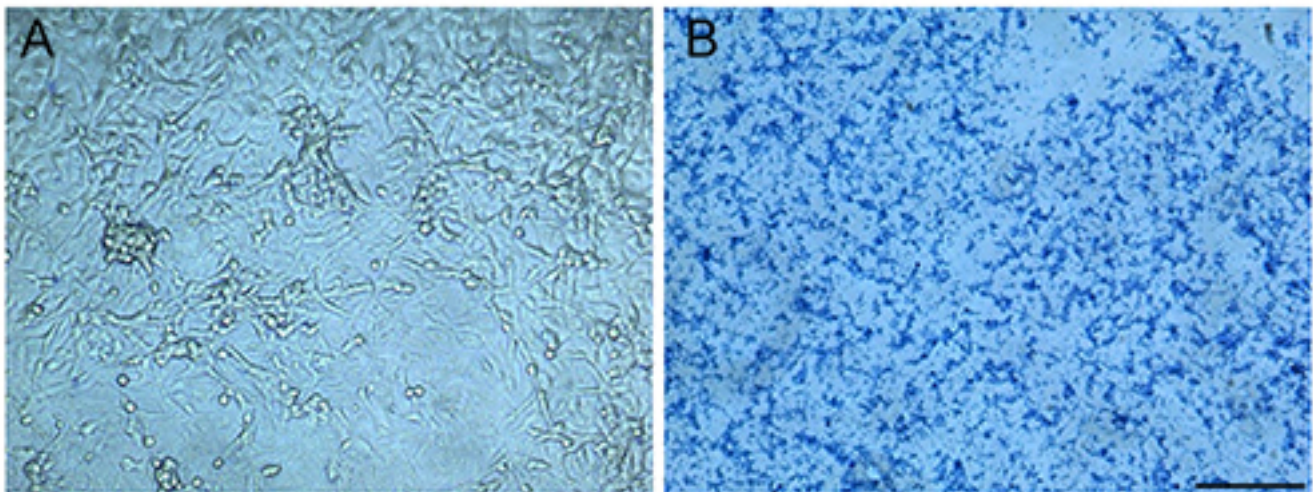


Figure 2. Tumor cell monolayers and ECM plated on CSM slide wells. Photomicrographs of slide wells prepared with (A) confluent U-87MG glioma cell monolayers, or (B) ECM proteins extracted from confluent U-87MG stained with Coomassie blue dye. Bar = 200 μ m. [Click here for a larger version of this figure.](#)

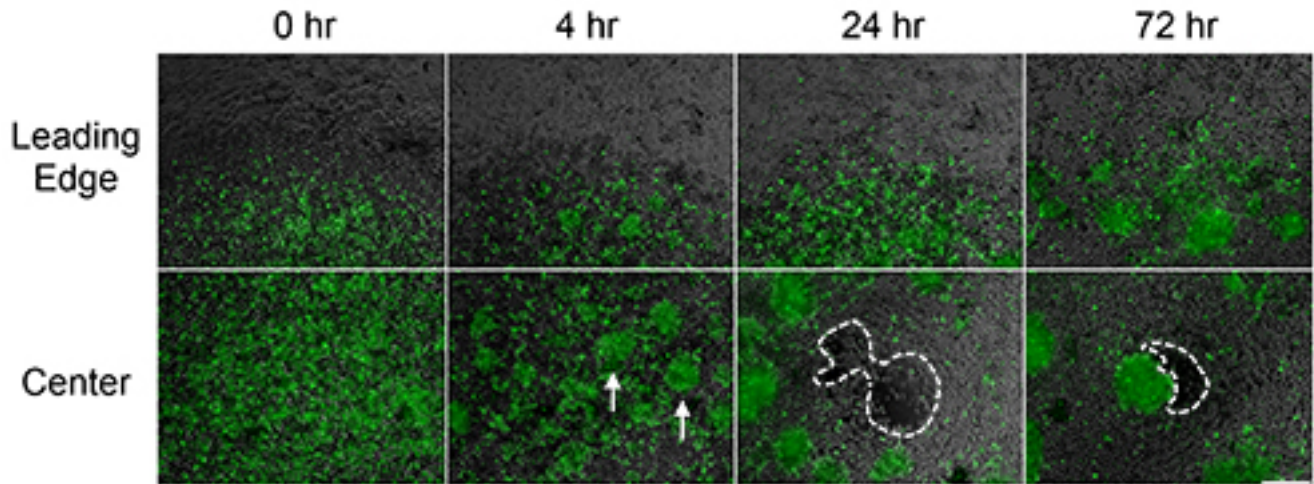


Figure 3. Migration and cytotoxicity of RRV-EMD transduced lymphocytes at the center and leading edge of cell deposit over time. Fluorescent photomicrographs taken at various times at the leading edge and at the center of alloCTL-RRV-EMD following sedimentation on a monolayer of adherent U-87MG glioma cells. Effector alloCTL seeded as single cells, form spherical clusters within 4 hr (white arrows) of placement. Single fluorescently-labeled CTL have migrated from the center of the well as time progresses. After 24 hr, empty cell patches in the adherent monolayer are visible presumably due to alloCTL cytolysis of the tumor target cells (see area within dashes). Bar = 200 μ m. [Click here for a larger version of this figure.](#)

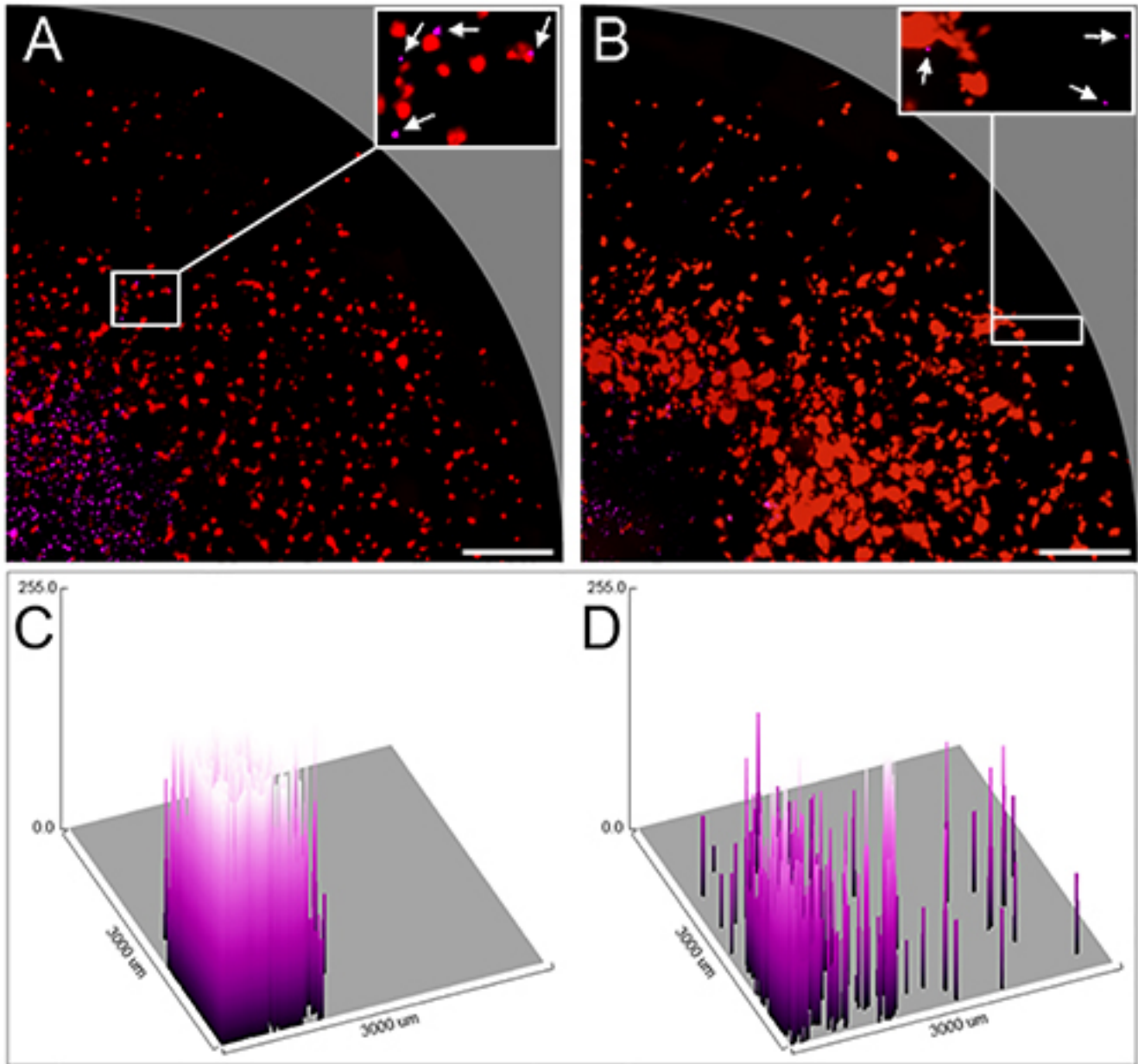


Figure 4. Radial migration of murine alloCTL stained with eFluor 670 on mStrawberry-labeled glioma cells shown at 1 and 48 hr. Fluorescent photomicrographs of one quadrant of the same well at (A) 1 hr and (B) 48 hr after sedimentation of fluorescently-labeled non-adherent alloCTL onto a monolayer of TU-2449 glioma cells. The low power photomicrographs reflect the area contained within one quadrant of the CSM well (radius 3 mm). At high power (A and B, insets) alloCTL (white arrows) are shown in proximity to or associated with individual tumor cells; one has a disintegrated appearance with fragmented nuclei and is apoptotic. (C and D) respective surface intensity fluorescence maps obtained using ImageJ software showing pixel values of the digitized purple fluorescent images in three-dimensional graphic form and placed on a grid representing the well radius of 3 mm. Bar = 500 μm. [Click here for a larger version of this figure.](#)

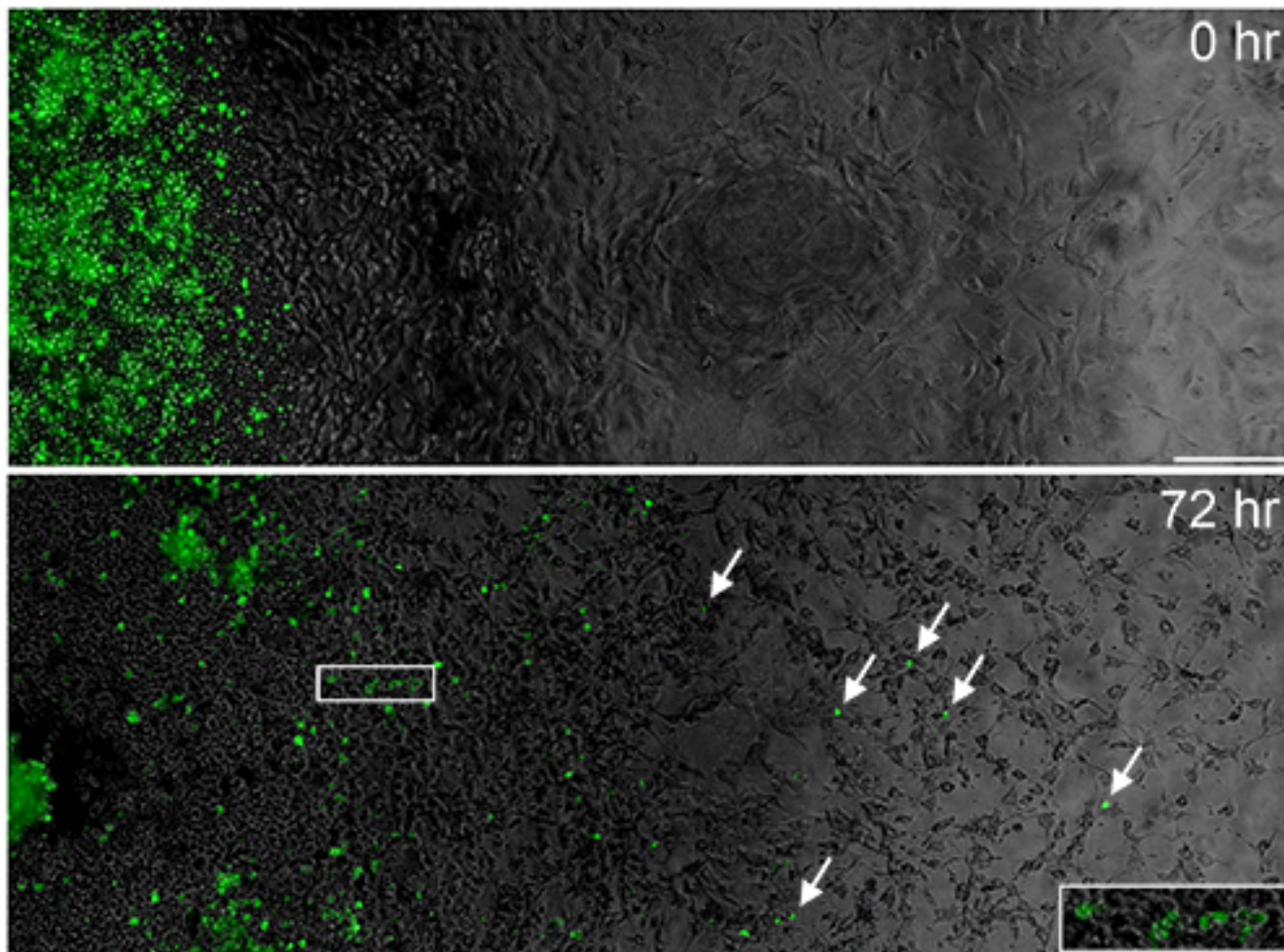


Figure 5. Migration of alloCTL and horizontal spread of RRV-EMD from transduced alloCTL to tumor cells. Fluorescent photomicrographs serially stitched together to cover the radius of the well using image editing software. Migration of RRV-EMD transduced alloCTL (white arrows) is shown on a monolayer of U-87MG tumor cells at 0 and 72 hr following sedimentation. RRV-EMD transduction of tumor cells in the monolayer is also apparent at 72 hr following addition of the EMD-transduced alloCTL, indicating that horizontal transmission of infective RRV from lymphocytes to tumor cells has occurred (white box, and inset). Bar = 200 μ m. [Click here for a larger version of this figure.](#)

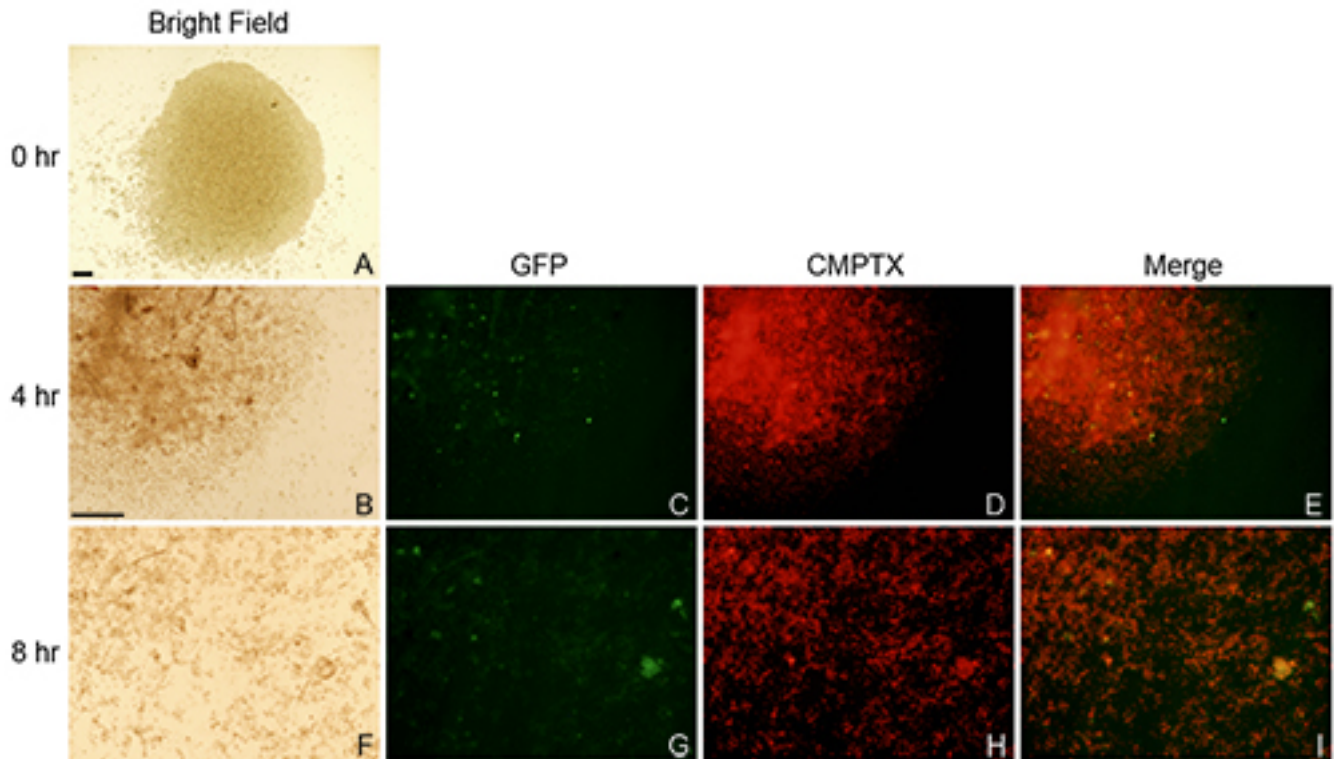


Figure 6. Radial migration of alloCTL transduced with RRV-EMD and stained with CellTracker Red CMPTX. Cells were sedimented onto ECM extracts derived from MDA-MB-231BR cells. Migration of alloCTL was imaged by bright field light microscopy at 0, 4 and 8 hr (A, B, F column 1, respectively). Fluorescent images of the CMPTX (red) labeled alloCTL (C, G, column 2), the RRV-EMD (green) transduced alloCTL (D, H, column 3), and the merged images (E, I, column 4) are shown at 4 and 8 hr. Bars = 200 μ m; Bar shown in B applicable to images C-I. [Click here for a larger version of this figure.](#)

Discussion

Tumor cells in a single cell suspension were pipetted into the wells of a Teflon-masked slide. The cells were allowed to adhere and then formed monolayers in a humidified 5% CO₂, 37°C incubator (Figure 1A). Established monolayers or ECM proteins derived from the monolayer could be harvested for these assays (Figure 1B). Effector T lymphocytes labeled with vital fluorescent dyes or transduced with vectors coding for EMD were seeded into the center of the well using a CSM. The ability of non-adherent effector T lymphocytes to migrate on the monolayer or ECM proteins over time was then evaluated and quantified with light and fluorescence microscopy. Here, we evaluated the migration and cytotoxicity of non-adherent effector alloCTL on a monolayer of partially-relevant target U-87MG glioma cells (Figures 3 and 5). These target cells, displaying only some of the Human Leukocyte Antigen (HLA) molecules (HLA-A2, B44) found on the original stimulators, were used to reduce the potent lytic activity that would be displayed by the alloCTL to the relevant 13-06-MG target cells (HLA-A1,2 and B44,57). We also observed the mobility of the alloCTL on ECM harvested from a monolayer of MDA-MB-231BR breast tumor cells (Figure 6). The alloCTL were generated by one-way MLTR according to methods previously published⁹. Effector alloCTL were harvested 4-5 days after one-way MLTR and transduced with RRV-GS4-EMD (Figures 3 and 5) or RRV-ACE-EMD (Figure 6)^{10,11}. Higher transduction levels were achieved with the GS4 vector utilizing a Gibbon ape leukemia virus envelope than with the amphotropic ACE vector. Using this radial migration assay, we noted that both transduced and nontransduced fluorescently-labeled alloCTL had migratory capacity. We also demonstrate that they retain their ability to be cytotoxic after undergoing manipulations for RRV transduction.

The ability of murine alloCTL to migrate was also assessed (Figure 4). alloCTL sensitized to haplotype H-2b/k displayed by TU-2449 cells were stained with eFluor 670 (purple) and a migration assay was performed using TU-2449 transduced with CMV-Straw-IRES-FLUC2 (red). When using fully relevant target, a lower number of alloCTL effector cells were seeded to prevent rapid lysis of the tumor cell targets. Using 1 hr as a baseline, T cells are largely localized at high density in the center of the well as a single cell suspension. The 48 hr micrographs show extensive migration of T cells toward the outer edge of the well and clustering of the alloCTL is readily apparent with destruction of the tumor cells at the site of their initial deposit. Proliferation of the TU-2449 cells is evidenced as the mStrawberry labeled cells increase in density over the well. This is better seen in surface fluorescence plots that were generated to visualize the distribution of purple cells in the wells (Figure 4, bottom panel). AlloCTL mobility is much more evident in the well at 48 hr compared to the 1 hr baseline. Similar to what was seen in the assays utilizing human alloCTL and glioma cells, a clearance of the tumor cells around the area of the initial deposit of effectors is noticeable at 48 hr, suggesting lysis of the tumor target cells.

A critical step in this assay is the growth of healthy monolayers and subsequent harvest of 'skeletal' ECM. Seeding of the tumor cells at 2.5 – 5.0 x 10⁴ cells per well, according to step 1.9 above, usually resulted in a roughly even monolayer for the tumor cell types we used. We found it crucial to allow the tumor cells to adhere at RT, otherwise the convection that occurs at 37 °C will push the cells toward the center of the wells. As well, pre-coating of the wells with poly-D-lysine and/or an ECM protein such as fibronectin or collagen can greatly increase success

rate. Additionally, we had better success with these assays using monolayer-derived 'skeletal' ECM than with individual ECM components (*i.e.*, fibronectin, collagen), which proved much less reliable. It is important to experiment with the number of non adherent cells to deposit through the sedimentation manifold as well, and if using a pure cell type, one might theoretically be able to define a motility coefficient with this assay. Because the well volume is small and some evaporation of medium occurs, the monolayer needs to be replenished daily with fresh medium. Media replacement also prevents accumulation of toxic lactate as the cells grow and divide. Failure to cultivate a healthy monolayer can result in shedding of the monolayer or ECM from the well surface.

The Coomassie blue stained ECM proteins derived from the U-87MG glioma cell line according to step 1.13 above are shown as a visual example of the adherent substrate layer left behind after digestion with Triton X-100 (**Figure 1B**). ECM production from a breast carcinoma cell line, MDA-MB-231BR cells, often was patchy and thin, resulting in an ECM layer that was more poorly adherent and sometimes lifted from the slide during the assay. The ECM protein adherence to the slide improved when tumor cells were maintained as confluent monolayers for 1-2 days before digestion. Throughout the process, maintenance of the Teflon seal surrounding the well was also important. Keeping the volume low and minimizing exposure of the Teflon to the Triton-X100 solution mitigated damage to the integrity of the Teflon seal.

One adaptation of this protocol might be use of a three dimensional extracellular matrix harvested from sections of OCT embedded tumor tissue¹⁴. However, it should be noted that the distance from the flat bottomed well to the slide surface is only 1 mm; thus, sections exceeding this thickness may be disrupted by manifold placement. Also, a method would need to be devised for making a slight burr hole in the tissue to accept the droplet of medium containing the non-adherent cells.

Preparation of a well-dispersed single cell suspension of the effector T lymphocytes in advance of sedimentation was also imperative. Gentle titration of the non-adherent T cells to disperse aggregates to a single cell suspension was an essential step right before loading the alloCTL into the channels of the CSM. Use of non-enzymatic cell dissociation buffers should be employed if necessary. Further, the density of effector lymphocytes should be around $1.0 - 2.0 \times 10^5$ cells/ μ l for sedimentation, as described in step 2.8 above. Low cell numbers may result in no sedimentation, while higher cell numbers can cause a large deposit that is easy to disrupt when moving the slide. It is also recommended that the serum concentration in the medium be at least 10% to provide adequate surface tension of the positive meniscus that reduces the possibility of spillover.

An inverted light microscope with fluorescence imaging capabilities and a 4x or 10x objectives is optimal for this assay. The time points for imaging can be determined according to individual experimental inquiries and cell types. The non-adherent CTL in particular migrate from the center of sedimentation toward the edge of the well more quickly on ECM proteins (4-8 hr) than over a cell monolayer (12-72 hr). Partially MHC relevant target cells were preferable to relevant targets for our alloCTL assay to encourage the visualization of motility and reduce cell-mediated cytolysis of the monolayers before significant migration can occur; use of a low effector to target ratio also slows the lysis. The use of partially-matched targets allows for better visualization of RRV transmission to the tumor cells as well.

Use of an inverted microscope affords multiple advantages over an upright scope. An inverted scope allows for imaging through the humidified chamber so that slides do not have to be disturbed, while also maintaining a sterile environment for the cells. Also, imaging through the chamber provides a barrier between the specimen and the technician, allowing for adherence to biosafety level II (BSL II) guidelines when working with human-derived tissue¹⁵.

If using an upright scope, the highest magnification achievable without disturbing the positive meniscus of the well is 20x. Unfortunately, use of a coverslip, or optics kit accessories to the cell sedimentation manifold, is not recommended, as the disruption to the meniscus typically results in the spreading of the sedimented non-adherent cells throughout the well. Imaging over long periods of time may require careful addition of medium to each well to replace that lost to evaporation, although this is more likely to be required during time-lapse imaging.

This protocol is distinct from methods that measure horizontal cell migration of adherent cells in Zigmond Chambers^{16,17}, the design of which would not allow for the visualization of non-adherent cell migration. Other assays that evaluate horizontal migration toward a chemotactic gradient through a substrate such as agar are generally used to study migration of one cell type¹⁸⁻²⁰. Use of the CSM provides several advantages to these methods as well as methods that measure vertical migration/invasion of cultured cells, such as in Boyden chambers or Matrigel transwell plates. First, cell-cell contact allows for a determination of target-effector cell interaction and injury by effector cells. The cytolytic ability of alloCTL-RRV-EMD initially stimulated by one-way MLTR with stimulator 13-06-MG tumor cells to the partially MHC-matched U-87MG cell line is evident in the center of the monolayer at 24 and 72 hr following sedimentation (**Figures 3 and 5**, dashed lines). As well, the degradation of TU-2449 cells by murine alloCTL is visible at 48 hr post-sedimentation (**Figure 4**). The monolayer is obliterated at the center of alloCTL deposit, but occurs more slowly over the remainder of the monolayer, owing either to the overlap in HLA expression of 13-06-MG and U-87MG in the assays with human cells²¹ or the low starting number of effector cells for the murine glioma. Also, the effector to target density is reduced as the effector alloCTL migrate away from the sedimentation site. In addition to migration and cytolysis, this protocol can be used to visualize the transfer of virus encoding fluorescent proteins. Here, transfer of RRV coding for EMD from the alloCTL to the tumor cells is evident after 72 hr (**Figure 5**, inset).

The CSM was suitably designed for examining non-adherent cell mobility on adherent cells. It's design allowed for minimal disruption of the nonadherent cells with the adherent cell monolayer when the manifold was removed. Additionally, the center of sedimentation within the Teflon masked slide is identical in each well of the manifold allowing for reduced variability between experimental replicates. However, other options such as glass cylinders, cloning rings, or other machined devices could be validated for similar purpose.

A limitation of this model is that migration can only be assessed *in vitro*, which may not be truly reflective of the *in vivo* migration. Another limitation is that chemokine/chemokine receptor gradients cannot be established using the model. While interactions of immune cells with ECM or individual tumor cells may still occur and depend on what those cells secrete or express, this motility assay would not answer questions on whether the non-adherent cells will migrate specifically to or away from isolated factors.

An advantage of this assay is the ability to determine if a population of non-adherent cells maintain migratory functionality if the lymphocytes have or have not been transduced. In our example, the transduced subpopulation is visible through EMD protein expression, and it is clear that migratory functionality is maintained in this subpopulation. A wider application might be to test the effects of various concentrations of agents or

drugs that might affect non-adherent immune cell migration. Also, other hematopoietic cells might be tested for mobility on various substrates or adherent cells derived from normal tissue. Finally, although it is not done here, seeding a combination of adherent cell types, *i.e.*, stromal cells or dendritic cells with tumor, may provide analyses reflective of more complex *in vivo* environments.

Disclosures

The authors declare they have no competing financial interests.

Acknowledgements

Supported in part by NIH R01 CA121258, R01 CA125244, R01 CA154256, NIH/NCATS UCLA CTSI Grant Number UL1TR000124, USAMRMC W81XWH-08-1-0734, and the Joan S. Holmes Memorial Research Fund. MJH and GCO received supported from the Joan S. Holmes Memorial Postdoctoral Fellowship at UCLA. The CSM device was obtained from Creative Scientific Methods: www.creative-sci.com. The lentiviral vector was received from the UCLA Vector Core, which is supported by CURE/P30 DK041301.

References

- Hwang, J. H., Smith, C. A., Salhia, B., Rutka, J. T. The role of fascin in the migration and invasiveness of malignant glioma cells. *Neoplasia*. **10**, (2), 149-159 (2008).
- Valster, A., *et al.* Cell migration and invasion assays. *Methods*. **37**, (2), 208-215 (2005).
- Berens, M. E., Rief, M. D., Loo, M. A., Giese, A. The role of extracellular matrix in human astrocytoma migration and proliferation studied in a microliter scale assay. *Clin Exp Metastasis*. **12**, (6), 405-415 (1994).
- Osawa, H., Smith, C. A., Ra, Y. S., Kongkham, P., Rutka, J. T. The role of the membrane cytoskeleton cross-linker ezrin in medulloblastoma cells. *Neuro-oncology*. **11**, (4), 381-393 (2009).
- Berens, M. E., Beaudry, C. Radial monolayer cell migration assay. *Methods Mol Med*. **88**, 219-224 (2004).
- Giese, A., Rief, M. D., Loo, M. A., Berens, M. E. Determinants of human astrocytoma migration. *Cancer Res*. **54**, (14), 3897-3904 (1994).
- Vlodavsky, I., Levi, A., Lax, I., Fuks, Z., Schlessinger, J. Induction of cell attachment and morphological differentiation in a pheochromocytoma cell line and embryonal sensory cells by the extracellular matrix. *Dev Biol*. **93**, (2), 285-300 (1982).
- Hulkower, K. I., Herber, R. L. Cell migration and invasion assays as tools for drug discovery. *Pharmaceutics*. **3**, (1), 107-124 (2011).
- Hickey, M. J., *et al.* Implementing preclinical study findings to protocol design: translational studies with alloreactive CTL for gliomas. *Am J Transl Res*. **4**, (1), 114-126 (2012).
- Tai, C. K., Wang, W. J., Chen, T. C., Kasahara, N. Single-shot, multicycle suicide gene therapy by replication-competent retrovirus vectors achieves long-term survival benefit in experimental glioma. *Mol Ther*. **12**, 842-851 (2005).
- Logg, C. R., Baranick, B. T., Lemp, N. A., Kasahara, N. Adaptive evolution of a tagged chimeric gammaretrovirus: identification of novel cis-acting elements that modulate splicing. *J Mol Biol*. **369**, (5), 1214-1229 (2007).
- Koya, R. C., *et al.* Kinetic phases of distribution and tumor targeting by T cell receptor engineered lymphocytes inducing robust antitumor responses. *Proc Nat Acad Sci USA*. **107**, (32), 14286-14291 (2010).
- Zumwalde, N. A., Domae, E., Mescher, M. F., Shimizu, Y. ICAM-1-dependent homotypic aggregates regulate CD8 T cell effector function and differentiation during T cell activation. *J Immunol*. **191**, (7), 3681-3693 (2013).
- Campbell, C. B., Cukierman, E., Artym, V. V. 3-D extracellular matrix from sectioned human tissues. *Curr Protocol Cell Biol*. **62**, (Unit 19), 11-20 (2014).
- Prevention, C. fd. C. a *Biosafety in Microbiological and Biomedical Laboratories (BMBL)*. Health and Human Services (2009).
- Zigmond, S. H. Ability of polymorphonuclear leukocytes to orient in gradients of chemotactic factors. *J Cell Biol*. **75**, (2 Pt 1), 606-616 (1977).
- Alstergren, P., *et al.* Polarization and directed migration of murine neutrophils is dependent on cell surface expression of CD44. *Cell Immunol*. **231**, (1-2), 146-257 (2004).
- Nelson, R. D., Quie, P. G., Simmons, R. L. Chemotaxis under agarose: a new and simple method for measuring chemotaxis and spontaneous migration of human polymorphonuclear leukocytes and monocytes. *J Immunol*. **115**, (6), 1650-1656 (1975).
- Yin, X., Knecht, D. A., Lynes, M. A. Metallothionein mediates leukocyte chemotaxis. *BMC Immunol*. **6**, (12), 21 (2005).
- Hadjout, N., Laevsky, G., Knecht, D. A., Lynes, M. A. Automated real-time measurement of chemotactic cell motility. *Biotechniques*. **31**, (5), 1130-1138 (2001).
- Zhang, J. G., *et al.* Tumor antigen precursor protein profiles of adult and pediatric brain tumors identify potential targets for immunotherapy. *J Neuro-oncol*. **88**, 65-76 (2008).